Proceedings of the XII International Symposium on Dynamic Problems of Mechanics (DINAME 2007),
P.S.Varoto and M.A.Trindade (editors), ABCM, Ilhabela, SP, Brazil, February 26 - March 2, 2007

Multiobjective Optimization of Active-Passive Damping Treatments using Genetic Algorithms

Marcelo A. Trindade[1]

[1] Department of Mechanical Engineering, São Carlos School of Engineering, University of São Paulo, Av. Trabalhador São-Carlense, 400, São Carlos-SP, 13566-590, Brazil, E-mail: trindade@sc.usp.br

Abstract: Several active-passive damping treatments using viscoelastic and piezoelectric materials have been studied in the last decade. The main motivation of such hybrid damping mechanisms is that they combine the reliability, low cost and robustness of viscoelastic damping treatments and the high performance, modal selective and adaptive piezoelectric active control. However, active-passive damping performance is highly dependent on the relative positions of viscoelastic and piezoelectric materials. This work presents a geometric and topological optimization of active-passive damping treatments, consisting of a viscoelastic layer, a constraining layer, a spacer layer and a set of piezoelectric actuators. The modeling is performed using a piezoelectric sandwich/multilayer beam finite element model in which the viscoelastic material frequency-dependence is accounted for using the Anelastic Displacement Fields model. The resulting model is then reduced using a two-step modal reduction and applied to a limited-input optimal control strategy to evaluate the resulting active-passive modal damping factors. An aggregated weighted min-max approach for the multiobjective optimization is used to establish a set of optimal cases for different cost weighting factors, leading to a set of trade-off surfaces. Results show that a considerable improvement of damping performance is achievable with a controlled increase in the mass of the structure.

Keywords: Active-passive damping, viscoelastic materials, piezoelectric materials, optimization, genetic algorithms

INTRODUCTION

Several research works published in the last decade have shown the advantages of combining the standard free layer and constraining layer viscoelastic damping treatments with some type of distributed active control to reduce the structural vibration amplitudes. The viscoelastic damping treatments offer a reliable, low cost and robust solution for vibration damping and are already widely used in several industries. On the other hand, studies on the application of distributed active control using piezoelectric actuators for real structures has seen a considerable growth in recent years. Although a purely active control is normally not robust enough for industrial applications, it can provide high performance, modal selective and adaptive solutions for narrow frequencies ranges. Aiming to improve passive damping performance or reduce the required weight increase, a number of research groups proposed hybrid active-passive damping treatments configurations combining both viscoelastic and piezoelectric materials in the structural design (Lam, Inman and Saunders, 1998; Trindade and Benjeddou, 2002).

Depending on the relative positions of the passive damping layers and the active piezoelectric actuators, the active and passive damping mechanisms can work separately or simultaneously. The most studied configuration consists of replacing or augmenting the elastic constraining layer of a Passive Constrained Layer (PCL) damping treatment by an active piezoelectric actuator, leading to the so-called Active Constrained Layer (ACL) damping treatment (Azvine, Tomlinson and Wynne, 1995; Baz and Ro, 1994; Huang, Inman and Austin, 1996). Alternative configurations to ACL, mainly separating the passive treatment of the active piezoelectric actuators, were later proposed (Lam, Inman and Saunders, 1998; Trindade and Benjeddou, 2002). It was shown that, although each configuration has its advantages, the active damping performance is very much dependent on the transmissibility between piezoelectric actuators and host beam. Hence, ACL design can only be an interesting design when active and passive damping are designed to operate complementarily. However, other design configurations are still to be validated.

This work presents a geometric and topological optimization of active-passive damping treatments, consisting of a viscoelastic layer, a constraining layer, a spacer layer and a set of piezoelectric actuators. Thus, most of the previously proposed active-passive damping treatment configurations are accounted for. The main objective of the study is to evaluate relevant design variables and obtain potential operational ranges for each active-passive damping treatment. The modeling is performed using a piezoelectric sandwich/multilayer beam finite element model in which the viscoelastic material frequency-dependence is accounted for using the Anelastic Displacement Fields model. The resulting model is then reduced using a two-step modal reduction and applied to a limited-input optimal control strategy to evaluate the resulting active-passive modal damping factors. An aggregated weighted min-max approach for the multiobjective optimization is used to establish a set of optimal cases for different cost weighting factors, leading to a set of trade-off surfaces. An optimization strategy based on Genetic Algorithms (GA) is used (Houck, Joines and Kay, 1995).

FINITE ELEMENT MODEL

A finite element (FE) model for piezoelectric-viscoelastic laminate beams, based on a classical sandwich theory with laminate faces, was developed in a previous work (Trindade, Benjeddou and Ohayon, 2001a). The electromechanical coupling in the piezoelectric layers is accounted for through a static condensation of the stiffness matrix, in the case of unknown electric degrees of freedom (dof) induced in piezoelectric sensors, and through the evaluation of an equivalent load vector due to prescribed electric dof applied to piezoelectric actuators. Hence, the FE model is written in terms of mechanical dof only but fully accounts for piezoelectric sensors and actuators. The temperature and frequency dependence of the viscoelastic material properties is represented using the anelastic displacement fields (ADF) model (Lesieutre and Bianchini, 1995), which is based on the inclusion of internal variables to model the relaxation of the viscoelastic material.

The ADF model is based on a separation of the viscoelastic material strains in an elastic part, instantaneously proportional to stress, and an anelastic (or dissipative) part, representing material relaxation. This is applied to the FE model by replacing the mechanical dof vector $\mathbf{q}$ by $\mathbf{q}^e = \mathbf{q} - \sum_i \mathbf{q}_i^d$ in the strain energy corresponding to the viscoelastic elements. $\mathbf{q}^e$ and $\mathbf{q}_i^d$ represent the dof vectors associated with the elastic and anelastic strains, respectively. Then a series of equations, describing the time-domain evolution of the dissipative dof $\mathbf{q}_i^d$, is added to the FE equations of motion such that

$$\mathbf{M}\ddot{\mathbf{q}} + \mathbf{D}\dot{\mathbf{q}} + (\mathbf{K}_e + \mathbf{K}_v^\infty)\mathbf{q} - \mathbf{K}_v^\infty \sum_i \mathbf{q}_i^d = \mathbf{F}_m + \mathbf{F}_e \tag{1}$$

$$\frac{C_i}{\Omega_i}\mathbf{K}_v^\infty \dot{\mathbf{q}}_i^d + C_i \mathbf{K}_v^\infty \mathbf{q}_i^d - \mathbf{K}_v^\infty \mathbf{q} = \mathbf{0} \tag{2}$$

where $\mathbf{M}$ is the mass matrix, $\mathbf{D}$ is a viscous damping matrix, $\mathbf{F}_m$ is a mechanical forces vector and $\mathbf{F}_e$ is the piezoelectric forces vector. $\mathbf{K}_v^\infty$ is the unrelaxed (or instantaneous) stiffness matrix of the viscoelastic elements and $\mathbf{K}_e$ is the stiffness matrix of the remaining elements in the structure (elastic and piezoelectric). $\mathbf{K}_v^\infty$ is assumed to be proportional to the viscoelastic material unrelaxed shear modulus G_∞, such that $\mathbf{K}_v^\infty = G_\infty \bar{\mathbf{K}}_v$. The unrelaxed shear modulus is written in terms of the static (or relaxed) shear modulus G_0 as $G_\infty = G_0(1 + \sum_i \Delta_i)$. The ADF parameters $C_i = (1 + \sum_i \Delta_i)/\Delta_i$, G_0, Δ_i and Ω_i are evaluated by curve-fitting of the measurements of the complex shear modulus $G^*(\omega)$, represented as a series of functions in the frequency-domain (Lesieutre and Bianchini, 1995)

$$G^*(\omega) = G_0 + G_0 \sum_i \Delta_i \frac{\omega^2 + \mathrm{j}\omega\,\Omega_i}{\omega^2 + \Omega_i^2} \tag{3}$$

Notice that since viscoelastic materials properties are also dependent on temperature, the ADF parameters G_0, Δ_i and Ω_i should be evaluated for each temperature of interest. Equation (3) is well adapted to curve-fit complex modulus of viscoelastic materials with strong frequency dependence. Nevertheless, modern viscoelastic materials tend to be less frequency-dependent so as to maintain a high loss factor over a wide frequency-range of interest, and consequently being more effective in damping vibrations. For such materials, a larger number of series terms must be used to provide a satisfactory curve-fit of complex modulus frequency dependence. Since there is one system of equations (2) for each ADF series, this model can considerably increase the system dimension.

It is worthwhile to notice also that in the case of a structure partially covered with the viscoelastic treatment, the viscoelastic stiffness matrix $\mathbf{K}_v^\infty$ will possess a number of rigid body modes, corresponding to the FE dof of the non-treated parts of the structure. The rigid body modes of $\mathbf{K}_v^\infty$ can be eliminated through a modal decomposition $\mathbf{q}_i^d = \mathbf{T}_d \hat{\mathbf{q}}_i^d$, such that $\Lambda_d = \mathbf{T}_d^T \mathbf{K}_v^\infty \mathbf{T}_d$ and Eqs. (1) and (2) can be rewritten as

$$\mathbf{M}\ddot{\mathbf{q}} + \mathbf{D}\dot{\mathbf{q}} + (\mathbf{K}_e + \mathbf{K}_v^\infty)\mathbf{q} - \mathbf{T}_d \Lambda_d \sum_i \hat{\mathbf{q}}_i^d = \mathbf{F}_m + \mathbf{F}_e \tag{4}$$

$$\frac{C_i}{\Omega_i}\Lambda_d \dot{\hat{\mathbf{q}}}_i^d + C_i \Lambda_d \hat{\mathbf{q}}_i^d - \Lambda_d \mathbf{T}_d^T \mathbf{q} = \mathbf{0} \tag{5}$$

MODEL REDUCTION

A model reduction of the augmented system of equations (4) and (5) was recently proposed (Trindade, 2006) and it is briefly reviewed here. For more details, please refer to (Trindade, 2006). It consists in reducing the dissipative system (Eq. (5)) through the truncation of the dissipative modal basis $\mathbf{T}_d$. The choice of the retained dissipative modes is done by evaluating their projection onto an undamped modal basis $\mathbf{T}_e$, such that $\mathbf{T}_e^T \mathbf{M} \mathbf{T}_e = \mathbf{I}$ and $\mathbf{T}_e^T (\mathbf{K}_e + \mathbf{K}_v^\infty)\mathbf{T}_e = \Lambda_e$, and selection of a number of dissipative modes with higher projections. Since there are several alternatives to evaluate the projection onto a set of retained undamped modes, here it is chosen to quantify the overall importance of a dissipative mode by the norm of the projection onto each retained undamped mode. Hence, a so-called residual vector $\mathbf{r}$ is defined as

$$r_j = ||R_{jk}||, \text{ for } k \in \{N_k\} \tag{6}$$

where

$$\mathbf{R} = \Lambda_d \mathbf{T}_d^T \mathbf{T}_e \tag{7}$$

such that element R_{jk} represents the weighted residuals between viscoelastic dissipative mode $\mathbf{T}_d^j$ and undamped mode $\mathbf{T}_e^k$. Supposing that the majority of structural response energy is contained in the $\{N_k\}$ modes in $\mathbf{T}_e$, the selection of dissipative modes that contribute the most to the structural response may be performed through sorting of the residual vector $\mathbf{r}$. Notice that each element of $\mathbf{r}$ correspond to a column of $\mathbf{T}_d$, that is a viscoelastic dissipative mode. Thus, it is proposed to eliminate the dissipative modes from $\mathbf{T}_d$ corresponding to the smallest residuals r_j, which are thought to be those that contribute the least to the structural response. Therefore, the dissipative dof is approximated by $\mathbf{q}_i^d \approx \mathbf{T}_{dr}\hat{\mathbf{q}}_i^{dr}$. The reduced dissipative modal matrix $\mathbf{T}_{dr}$ contains thus only retained dissipative modes and $\hat{\mathbf{q}}_i^{dr}$ are their corresponding coordinates. Since the eigenvalues matrix is also reduced to Λ_{dr}, the residual matrix becomes $\mathbf{R}_r = \Lambda_{dr}\mathbf{T}_{dr}^T\mathbf{T}_e$.

Using the reduction of dissipative coordinates and the projection of the structural model, such that $\mathbf{q} = \mathbf{T}_e\hat{\mathbf{q}}$, Eqs. (4) and (5) can be rewritten as

$$\ddot{\hat{\mathbf{q}}} + \mathbf{T}_e^T\mathbf{D}\mathbf{T}_e\dot{\hat{\mathbf{q}}} + \Lambda_e\hat{\mathbf{q}} - \mathbf{R}_r^T\sum_i \hat{\mathbf{q}}_i^{dr} = \mathbf{T}_e^T\mathbf{F}_m + \mathbf{T}_e^T\mathbf{F}_e \tag{8}$$

$$\frac{C_i}{\Omega_i}\Lambda_{dr}\dot{\hat{\mathbf{q}}}_i^{dr} + C_i\Lambda_{dr}\hat{\mathbf{q}}_i^{dr} - \mathbf{R}_r\hat{\mathbf{q}} = \mathbf{0} \tag{9}$$

Notice that the structural model could also be reduced using its undamped modes $\mathbf{T}_e$. However, this is not done here, although writing the equations in terms of $\hat{\mathbf{q}}$ instead of $\mathbf{q}$ has some computational advantages. Notice that the reduced dissipative coordinates $\hat{\mathbf{q}}_i^{dr}$ contain now only those coordinates corresponding to selected dissipative modes according to their residual and, thus, matrices $\mathbf{R}_r$ and Λ_{dr} have a reduced dimension. This reduction can be specially important since each eliminated dissipative mode leads to a reduction of n dof, where n is the number of ADF series terms considered (generally at least 3).

In order to use this model for control design, Eqs. (8) and (9) are first rewritten in a state space form. Therefore, a state vector $\mathbf{x}$ is formed by an augmented vector $\bar{\mathbf{q}} = \text{col}\left(\hat{\mathbf{q}},\ \hat{\mathbf{q}}_1^{dr},\ \ldots,\ \hat{\mathbf{q}}_n^{dr}\right)$ and the time-derivative of the undamped modal coordinates vector $\dot{\hat{\mathbf{q}}}$. The time-derivatives of the dissipative coordinates $\hat{\mathbf{q}}_i^{dr}$ are not included in the state vector since these variables are massless. This leads to

$$\begin{aligned} \dot{\mathbf{x}} &= \mathbf{A}\mathbf{x} + \mathbf{B}\mathbf{u} + \mathbf{p} \\ \mathbf{y} &= \mathbf{C}\mathbf{x} \end{aligned} \tag{10}$$

where the perturbation vector $\mathbf{p}$ is the state distribution of the mechanical loads $\mathbf{F}_m$, $\mathbf{B}$ is the control distribution vector, corresponding to the piezoelectric loads per unit control voltage $\mathbf{F}_e^*$ induced by the piezoelectric actuators, the control input vector $\mathbf{u}$ is composed by the control voltages applied to each piezoelectric actuator, and the output vector $\mathbf{y}$ is composed of the measured quantities, written in terms of the state vector $\mathbf{x}$ through the output matrix $\mathbf{C}$. The system dynamics is determined by the square matrix $\mathbf{A}$. These are

$$\mathbf{A} = \begin{bmatrix} \mathbf{0} & \mathbf{0} & \cdots & \mathbf{0} & \mathbf{I} \\ \frac{\Omega_1}{C_1}\mathbf{T}_{dr}^T\mathbf{T}_e & -\Omega_1\mathbf{I} & & \mathbf{0} & \mathbf{0} \\ \vdots & & \ddots & & \mathbf{0} \\ \frac{\Omega_n}{C_n}\mathbf{T}_{dr}^T\mathbf{T}_e & \mathbf{0} & & -\Omega_n\mathbf{I} & \mathbf{0} \\ -\Lambda_e & \mathbf{R}_r^T & \cdots & \mathbf{R}_r^T & -\mathbf{T}_e^T\mathbf{D}\mathbf{T}_e \end{bmatrix}$$

$$\mathbf{x} = \begin{bmatrix} \bar{\mathbf{q}} \\ \dot{\hat{\mathbf{q}}} \end{bmatrix} ;\ \mathbf{p} = \begin{bmatrix} \mathbf{0} \\ \mathbf{T}_e^T\mathbf{F}_m \end{bmatrix} ;\ \mathbf{B} = \begin{bmatrix} \mathbf{0} \\ \mathbf{T}_e^T\mathbf{F}_e^* \end{bmatrix} ;\ \mathbf{C} = \begin{bmatrix} \mathbf{C}_q\mathbf{T}_e & \mathbf{0} & \mathbf{C}_{\dot{q}}\mathbf{T}_e \end{bmatrix}$$

where $\mathbf{C}_q$ and $\mathbf{C}_{\dot{q}}$ are output matrices relative to the mechanical dof $\mathbf{q}$ and their derivatives $\dot{\mathbf{q}}$, respectively. Notice that, as internal variables, the dissipative coordinates are not observable.

The state space system (10) can be further reduced, using any state space reduction technique, in particular to eliminate the unobservable dissipative coordinates. This is done here using a truncation of the complex damped modal basis followed by the construction of an equivalent real-valued state space system, as briefly explained below. Further details on the state space modal reduction can be found in (Trindade, Benjeddou and Ohayon, 2001b).

By neglecting the contributions of viscoelastic relaxation modes and some elastic modes, related to eigenfrequencies out of the frequency-range considered, a complex-based modal reduction is applied to the state space system (10). This is done through a modal decomposition, such that the right and left eigenvectors of $\mathbf{A}$ are evaluated by $\mathbf{A}\mathbf{T}_r = \Lambda\mathbf{T}_r$ and $\mathbf{A}^T\mathbf{T}_l = \Lambda\mathbf{T}_l$ with $\mathbf{T}_l^T\mathbf{T}_r = \mathbf{I}$. The state vector is then approximated as $\mathbf{x} \approx \mathbf{T}_{rr}\mathbf{T}_c^{-1}\hat{\mathbf{x}}$, where $\mathbf{T}_{rr}$ is the matrix of retained right eigenvectors of $\mathbf{A}$ and $\mathbf{T}_c$ is the matrix of complex-to-real state transformation. Hence, the reduced state space system is rewritten as

$$\begin{aligned} \dot{\hat{\mathbf{x}}} &= \hat{\mathbf{A}}\hat{\mathbf{x}} + \hat{\mathbf{B}}\mathbf{u} + \hat{\mathbf{p}} \\ \mathbf{y} &= \hat{\mathbf{C}}\hat{\mathbf{x}} \end{aligned} \tag{11}$$

where $\hat{\mathbf{A}} = \mathbf{T}_c\mathbf{T}_{lr}^T\mathbf{A}\mathbf{T}_{rr}\mathbf{T}_c^{-1}$; $\hat{\mathbf{p}} = \mathbf{T}_c\mathbf{T}_{lr}^T\mathbf{p}$; $\hat{\mathbf{B}} = \mathbf{T}_c\mathbf{T}_{lr}^T\mathbf{B}$; $\hat{\mathbf{C}} = \mathbf{C}\mathbf{T}_{rr}\mathbf{T}_c^{-1}$ and, in this form, the new state variables $\hat{\mathbf{x}}$ represent the modal displacements and velocities.

OPTIMAL CONTROL DESIGN

A Linear Quadratic Regulator (LQR) control design is applied to the reduced state space system (11). The optimization is performed using the following cost function

$$J = \frac{1}{2}\int_0^\infty (\hat{\mathbf{x}}^T\mathbf{Q}\hat{\mathbf{x}} + \mathbf{u}^T\mathbf{R}\mathbf{u})\, dt, \tag{12}$$

subjected to Eq. (11). This leads to a linear state feedback control system such that $\mathbf{u} = -\mathbf{K}_g\hat{\mathbf{x}}$, where $\mathbf{K}_g = \mathbf{R}^{-1}\hat{\mathbf{B}}^T\mathbf{P}$ is the control gain matrix written in terms of $\mathbf{P}$, the solution of the following algebraic Riccati equation

$$\hat{\mathbf{A}}^T\mathbf{P} + \mathbf{P}\hat{\mathbf{A}} - \mathbf{P}\hat{\mathbf{B}}\mathbf{R}^{-1}\hat{\mathbf{B}}^T\mathbf{P} + \mathbf{Q} = \mathbf{0}. \tag{13}$$

The performance of such a controller is determined by the proper choice of the weight matrices $\mathbf{Q}$ and $\mathbf{R}$. Besides, it does guarantee that the designed control input $\mathbf{u}$ is feasible. However, the control voltage applied to the piezoelectric actuators must be limited by a maximum electric field to avoid depoling of the piezoelectric material. Therefore, it is proposed to use an iterative algorithm that allows the automatic adjustment of the input weight matrix $\mathbf{R}$ by means of a factor γ, such that $\mathbf{R} = \gamma\,\bar{\mathbf{R}}$. The state weight matrix $\mathbf{Q}$ and the factored input weight matrix are set to identity matrices of proper dimension $\mathbf{Q} = \mathbf{I}_{n\times n}$ and $\bar{\mathbf{R}} = \mathbf{I}_{m\times m}$, where n is the dimension of state matrix $\hat{\mathbf{A}}$ and m is the number of actuators.

GEOMETRIC AND TOPOLOGICAL OPTIMIZATION

A geometric and topological optimization is proposed in this section using a genetic algorithm combined with a multiobjective optimization strategy.

Problem statement and design variables

A clamped-clamped aluminum beam, with Young's modulus 70.3 GPa, density 2690 kg m^{-3}, length $L = 320$ mm and thickness $h_B = 1.5$ mm, is considered as the base beam to be treated. It is proposed to apply to the beam a hybrid active-passive damping treatment composed of three active piezoelectric actuators and one constrained layer viscoelastic damping treatment, as shown in Fig. 1. The passive viscoelastic damping treatment is composed of an aluminum constraining layer, a viscoelastic layer and an aluminum spacer (or stand-off) layer. Their geometrical properties are as shown in Fig. 1, such that $d = 40$ mm, $a = 70$ mm, $e = 15$ mm, $h_P = 0.5$ mm, $h_C = [0,2]$ mm, $h_V = [0,1]$ mm and $h_S = [0,2]$ mm. The thicknesses h_C, h_V and h_S of passive damping treatment layers are considered as design variables. The viscoelastic material 3M ISD112, with density 1000 kg m^{-3}, is considered for the damping layer and it is represented by three series of ADF parameters, such that $G_0 = 0.50$ MPa, $\Delta = [0.7456; 3.2647; 43.2840]$, $\Omega = [468.69; 4742.36; 71532.49]$ rad/s. The piezoelectric actuators are made of piezoceramic material PZT5H with the following properties: density 7500 kg m^{-3}, equivalent Young's modulus 65.5 GPa and piezoelectric stress constant $e = -23,2$ C m^{-2}. Only the first ten bending modes are retained in the modal reduction. A viscous modal damping factor of 0.1% is also considered to represent other sources of damping. The maximum voltage applied to the piezoelectric actuators is set to 200 V for the control design, leading to a maximum electric field of 400 V/mm.

Together with the analysis of passive damping treatment thicknesses, six different active-passive configurations are considered by changing the relative position of the piezoelectric actuators, as shown in Fig. 2. This is done by defining a topology parameter p such that the following configurations are considered:

- $p = 0$ – no piezoelectric actuators and therefore without active control (Fig. 2a);
- $p = 1$ – piezoelectric actuators bonded directly to the bottom surface of the base beam (Fig. 2b);

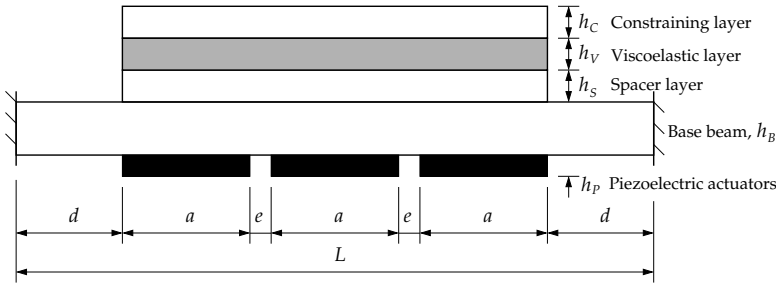

Figure 1 – Schematic representation of a clamped-clamped beam with active-passive damping treatment.

- $p = 2$ – piezoelectric actuators bonded between the base beam and the spacer layer, thus acting also as an additional spacer layer (Fig. 2c);
- $p = 3$ – piezoelectric actuators bonded between the spacer layer and the viscoelastic layer, hence acting on the base beam through the spacer layer (Fig. 2d);
- $p = 4$ – piezoelectric actuators bonded between the viscoelastic layer and the constraining layer, thus increasing the constraining layer thickness and acting on the base beam through the viscoelastic and spacer layers (Fig. 2e);
- $p = 5$ – piezoelectric actuators bonded to the external surface of the constraining layer, hence increasing the thickness and controlling the constraining layer (Fig. 2f).

Notice that, since bonding the piezoelectric actuators directly to the viscoelastic layer is not recommended, a very thin aluminum layer (thickness 1 mil or 0.0254 mm) is considered along the free surface of the viscoelastic layer in cases 3 and 4 (Figs. 2d and 2e).

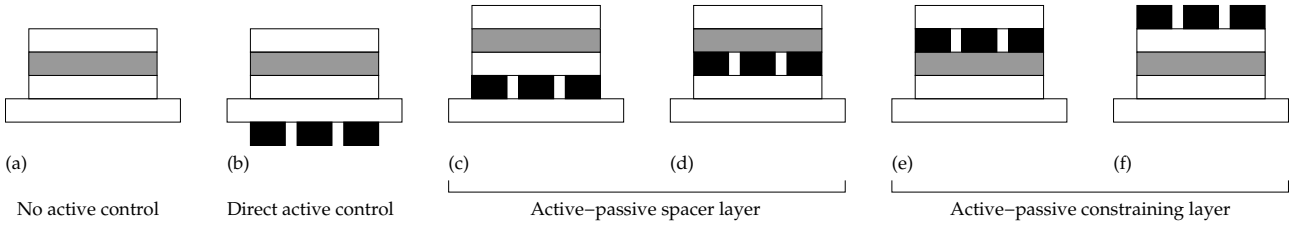

Figure 2 – Schematic representation of the six different topologies considered.

Objective function

The proposed objective is to maximize the overall damping for a given frequency-range while minimizing the mass added to the structure. This is done through the construction of a global performance index that combines an objective function J_d, corresponding the damping performance, and a penalty function J_m, corresponding to the added mass.

$$J_g = J_d - \beta J_m \; ; \; \beta > 0 \tag{14}$$

where the weighting factor β is used to establish trade-off surfaces. In particular, a small β is expected to lead to high damping performance at the cost of a considerable added mass, on the other hand, a large β restrains the added mass at the cost of poor damping performance. Notice that the global index J_g is defined such that a higher value means a better fit, in accordance with the basic concept of GA optimization.

The objective function J_d is defined as the arithmetic mean of the first five bending modes damping factors normalized by a maximum expected value ζ_{max}. Here, ζ_{max} was adjusted to 20% after some simulations.

$$J_d = \frac{1}{5\zeta_{max}} \sum_{i=1}^{5} \zeta_i \tag{15}$$

The penalty function J_m is defined as the relative increase in the structure mass normalized by a maximum expected value r_{max}. Here, r_{max} is considered to be 285%, which corresponds to the mass increase with the thicker viscoelastic, spacer and constraining layers, and the piezoelectric actuators.

$$J_m = \frac{1}{r_{max}} (m_T - m_B)/m_B \tag{16}$$

where m_T is the total mass of the treated beam and m_B is the mass of the base beam only. Notice that the total mass m_T is the sum of the masses of the base beam, the piezoelectric actuators, the spacer layer, the viscoelastic layer, and the constraining layer $m_T = m_B + m_P + m_S + m_V + m_C$ and, thus, is increased by the presence of the piezoelectric actuators ($p = [1,2,3,4,5]$) and by the increase in the spacer, viscoelastic and constraining layers thicknesses (h_S, h_V, h_C).

Optimization method

In the present work, a MATLAB implementation of the GA optimization algorithm, so-called *Genetic Algorithm for Optimization Toolbox* (GAOT), developed by Houck, Joines and Kay (1995), is used. GAs are search algorithms based on the "survival of the fittest" theory applied for a structured set of parameters (Goldberg, 1989). GAs have been often used for structural design optimization (Begg and Liu, 2000; Sadri, Wright and Wynne, 1999; Steffen, Rade and Inman, 2000) since, unlike conventional techniques, they do not require continuity or differentiability and, besides, they evaluate simultaneously a population of individuals (sets of parameters) and, hence, the probability of finding a local optima is reduced. The optimization using GA is an evolutionary process composed of three main steps: setup of an initial population, change of individuals parameters through mutation and crossover (reproduction), and selection of best individuals.

For the problem presented previously, the design variables p, h_S, h_V and h_C define the four parameters (or characteristics) of each individual of the population and, thus, each individual represents an active-passive damping treatment configuration. There are several strategies to setup an initial population. Here, the following strategy was retained: 1) evenly spaced vectors are constructed for each parameter, $[p] = [0,1,2,3,4,5]$, $[h_V] = [1,2,...,20]$ mil, $[h_C] = [h_S] = [0,0.1,...,2]$ mm; 2) vectors $[p]$, $[h_V]$, $[h_C]$ and $[h_S]$ are repeated to form corresponding augmented vectors with a given dimension N_{rp} (size of the random population); 3) each element of the augmented vectors (now with the same dimensions) are combined randomly to form a matrix with N_{rp} rows and 4 columns, where each row represents an individual with 4 parameters; 4) a set of N_{gs} potentially good solutions is included, so that the size of the initial population is $N = N_{rp} + N_{gs}$. In the present case, the random population is formed by $N_{rp} = 180$ individuals. Consequently, vectors $[p]$, $[h_V]$, $[h_C]$ and $[h_S]$ are repeated 30, 9, ˜9 and ˜9 times, respectively, which gives sufficient appearance frequency for each design variable value. In addition, $N_{gs} = 11$ potentially good solutions are included in the initial population. These are meant to represent four main configurations: the base beam with no treatment (optimal for $\beta \to \infty$); a relatively thick constraining layer ($h_C = 1.5$ mm) combined with a very thin viscoelastic layer ($h_V = 1$ mil) and a thin spacer layer ($h_S = 0.5$ mm) for the six topologies ($p = 0,1,2,3,4,5$); a relatively thick constraining layer ($h_C = 1.5$ mm) combined with a very thin viscoelastic layer ($h_V = 1$ mil) and without spacer layer ($h_S = 0$) for three topologies ($p = 0,1,5$); and the base beam with purely active control ($p = 1$, $h_V = h_C = h_S = 0$), that is without passive damping treatment. Then, the performance index J_g of each individual of the initial population is evaluated, for a given β, and associated with the corresponding individual.

Along a given number N_g of generations, the population evolves through a series of operations. First, a non-uniform mutation of N_m randomly selected individuals is performed, in which all parameters of one individual are randomly modified, respecting each parameter boundaries. The performance index of each individual is compared to that of its corresponding mutation and, if the mutation has a greater performance index, it replaces the original individual. Then, an arithmetic crossover (reproduction) of N_c pairs of randomly selected individuals is performed. A pair of new individuals (children) is generated corresponding to the two complementary linear combinations of each pair of original individuals (parents). The performance index is then evaluated for the children and, for each set parents/children, the pair of best solutions are retained. Finally, a selection of the best individuals is retained to the next generation. The selection is performed using a normalized geometric ranking for which a probability of being selected is assigned to each individual based on its performance ranking. In what follows, the following parameters were used $N_g = 15$, $N_m = 4$, $N_c = 27$.

RESULTS AND DISCUSSION

This section presents a series of optimal results obtained for several values of β and, then, each optimal configuration is analyzed in more detail. First, the weighting factor β for the added mass penalty function was varied through a wide range [0.001–1000] to identify ranges of interest. It was observed that a much narrower range [0.2–4.0] is sufficient to observe optimal ranges for each type of configuration. Figure 3 presents the evolution of population parameters, p, h_V, h_C and h_S, for $\beta = 0.2$. This figure was obtained by plotting a circle around each parameter pair found in the population, where the size of the circle represents the number of individuals possessing such parameter pair. These circles are then plotted for every generation in the same graph. It is then possible to observe that, through the generations, certain points (parameter pairs) start to accumulate individuals, meaning that all individuals are evolving to a certain set of characteristics. In Figure 3, for instance, it is possible to notice that, while the initial population is quite evenly distributed along the four design variables, all individuals converge to very thin viscoelastic and spacer layers, $h_V = 0.0254$ mm (1 mil) and $h_S = 0.1$ mm, relatively thick constraining layer $h_C = 1.7$ mm, and piezoelectric actuators placed between the viscoelastic and spacer layers (position $p = 3$). It can also be noted in Figure 3 that there is also a visible concentration of individuals around the position $p = 5$ for thinner constraining layer $h_C = 1.5$ mm and without spacer layer, configuration also known as APCL (active-passive constraining layer). However, these individuals later evolved to the optimal configuration.

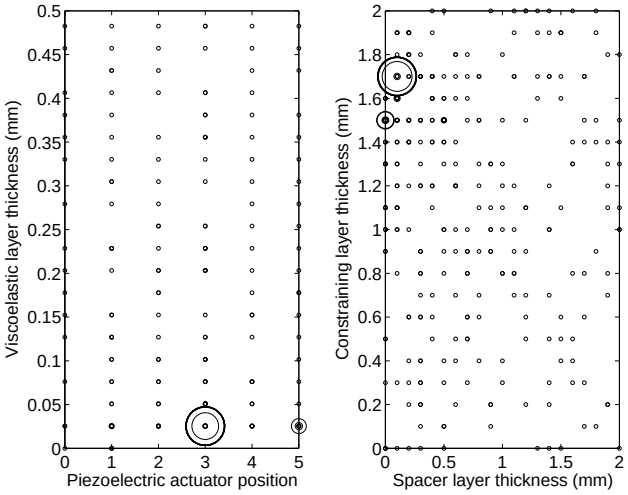

Figure 3 – Evolution of population parameters for $\beta = 0.2$.

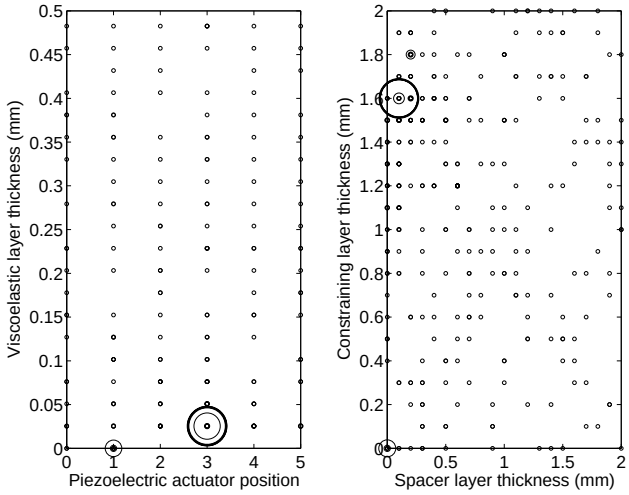

Figure 4 – Evolution of population parameters for $\beta = 0.5$.

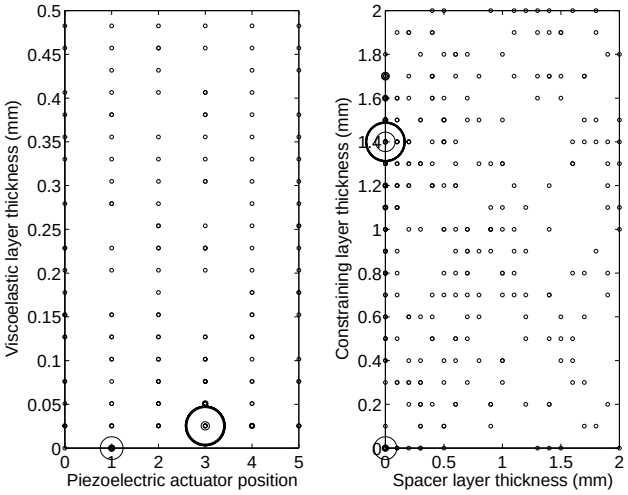

Figure 5 – Evolution of population parameters for $\beta = 0.8$.

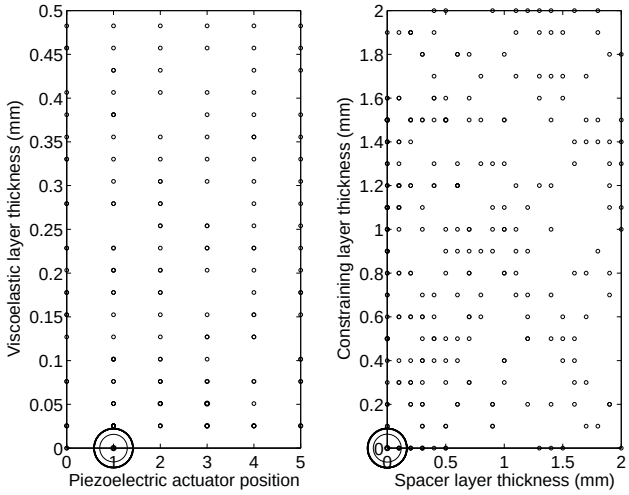

Figure 6 – Evolution of population parameters for $\beta = 1.0$.

Figure 4 shows the evolution of population parameters for $\beta = 0.5$. In this case, the optimal solution is obtained for $p = 3$, $h_V = 0.0254$ mm, $h_C = 1.6$ mm and $h_S = 0.1$ mm. Comparing with the previous case, the constraining layer is a little thinner. This is due to a greater weighting of the added mass. The same behavior can be observed in Figure 5, where the constraining layer is thinner $h_C = 1.4$ mm and the spacer layer is removed ($h_S = 0$).

A more considerable configuration change is obtained increasing β to 1.0. The evolution of population parameters for this case is shown in Figure 6. In this case, the piezoelectric actuators are bonded directly to the bottom surface of the base beam (position $p = 1$) and the passive damping layer is entirely removed ($h_V = h_C = h_S = 0$). This configuration represents a purely active damping of the base beam through the piezoelectric actuators and it is maintained as the optimal solution up to $\beta = 2.0$ (Figure 7). For greater values of β, this solution shall still be a good solution but it is not the optimal solution anymore. Indeed, Figure 8 shows that, for $\beta = 2.4$, the optimal configuration consists of purely passive damping, that is without piezoelectric actuators $p = 0$, with very thin viscoelastic, spacer and constraining layers, $h_V = 0.0254$ mm and $h_S = h_C = 0.1$ mm. The purely passive damping configuration remains the optimal solution for greater values of β. However, increasing the weight of the added mass penalty function, β, restrains more and more the thickness of the passive damping treatment. Hence, for $\beta = 3.4$, the spacer layer is removed ($h_S = 0$), as shown in Figure 9, and, for $\beta = 4.0$, both spacer and constraining layers are removed ($h_C = h_S = 0$), as shown in Figure 10, leading to a passive free layer damping. Although, for the sake of brevity, it is not shown here, continuous increase in β leads to reduction of the viscoelastic layer until the optimal solution reduces to the base beam only.

It is also worthwhile to notice that the optimal solution presented previously can be grouped in three main categories: 1) hybrid active-passive damping treatment (optimal up to $\beta = 0.8$); 2) purely active damping treatment (optimal from $\beta = 1.0$ to $\beta = 2.0$); and purely passive damping treatment (optimal from $\beta = 2.4$ to $\beta = 140$, from where the optimal

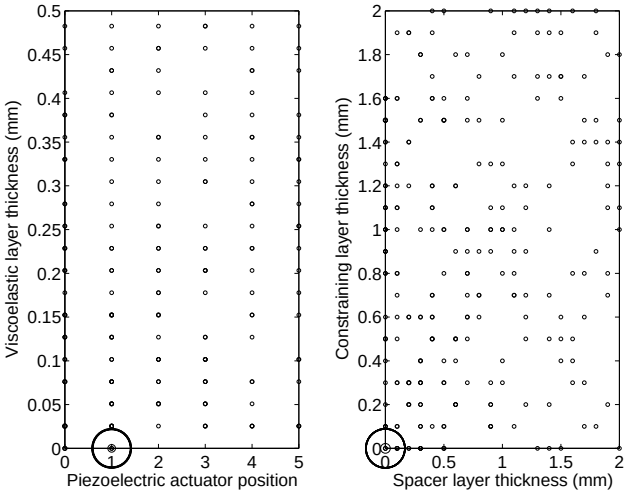

Figure 7 – Evolution of population parameters for $\beta = 2.0$.

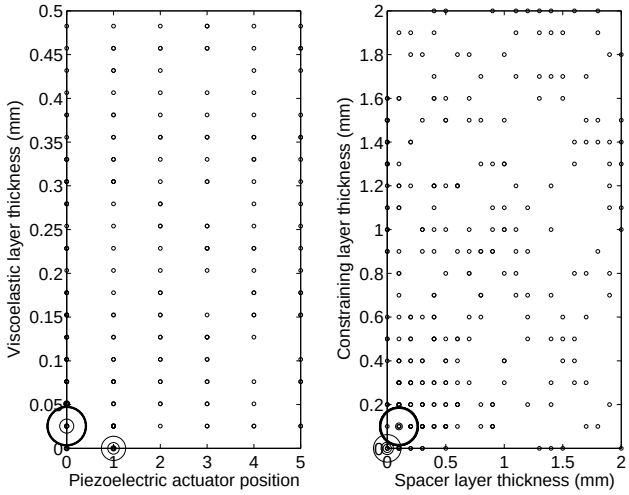

Figure 8 – Evolution of population parameters for $\beta = 2.4$.

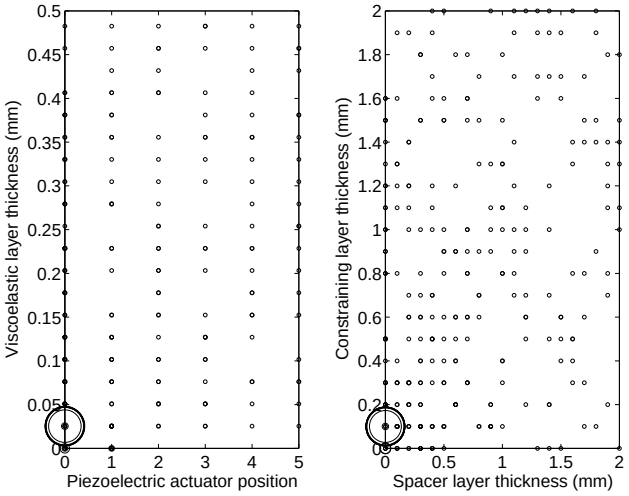

Figure 9 – Evolution of population parameters for $\beta = 3.4$.

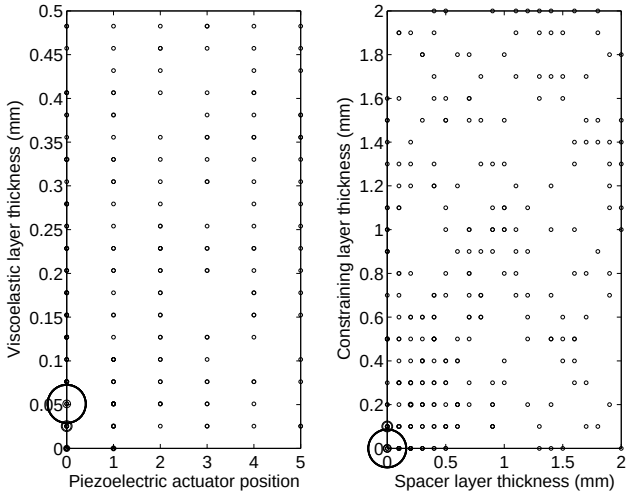

Figure 10 – Evolution of population parameters for $\beta = 4.0$.

solution is no treatment at all). These configurations with their variations are shown in Figure 11 together with the damping performance index J_d (solid) and the added mass penalty function J_m (dashed), as functions of the weight β. Since the added mass is a penalty function and for the sake of clarity, Figure 11 shows $1 - J_m$ instead of J_m. It can be noticed that for small values of β, e.g. $\beta = 0.2$, the damping performance index is near 1, meaning an average damping factor of approximately 20% (19.6%, actually), while the added mass penalty function is $J_m = 0.54$, leading to a mass increase of 153%. For the purely active damping configuration ($1.0 \leq \beta \leq 2.0$), the damping performance index is $J_d = 0.54$, meaning an average damping of 10.9%, while the added mass penalty function is $J_m = 0.21$, meaning a mass increase of 61%. For the purely passive damping configuration ($2.4 \leq \beta \leq 4.0$), the damping performance index drops to $0.24 \leq J_d \leq 0.29$, leading to an average damping factor of 5.8% for $\beta = 2.4$ and 4.9% for $\beta = 4.0$. On the other hand, the added mass penalty function is reduced to $0.037 \leq J_m \leq 0.003$, meaning a much smaller mass increase of 10% for $\beta = 2.4$ and 1% for $\beta = 4.0$.

In addition to the analysis of average damping performance, it is worthwhile analyzing separately the damping factor of the ten first bending modes for each active-passive damping configuration. This is done here for four configurations, namely the first active-passive damping treatment of Figure 11 (for $\beta = 0.2$), the purely active damping treatment (for $\beta = 1.0$), the passive constrained stand-off layer damping treatment (first passive damping treatment of Figure 11, for $\beta = 2.4$), and the passive free layer damping treatment (last passive damping treatment of Figure 11, for $\beta = 4.0$). The ten first damping factors for these selected configurations are shown in Figure 12, where configurations 1, 2, 3 and 4 refer respectively to active-passive damping, active damping, passive constrained layer damping, and passive free layer damping. One may notice that active-passive damping leads to high damping factors for all modes (minimum of more than 14% for modes 4 and 10). It is worthwhile noticing that an important part of these damping factors comes from the passive

damping treatment (up to the thin mark in each bar), meaning that even for open loop condition, or in the eventuality of control system malfunction, the structure is well damped. On the other hand, the purely active damping configuration lacks this open-loop damping threshold, but in closed-loop the piezoelectric actuators are able to effectively damp up to mode 7 (Figure 12). However, active damping factors of modes 8, 9 and 10 are much smaller (2%, 0.3% and 0.9%). From Figure 12, it is possible to notice that the much lighter purely passive damping treatments (selected configurations 3 and 4) still yield considerable damping factors for all ten bending modes (greater than 5.2% for constrained layer and greater than 4.7% for free layer).

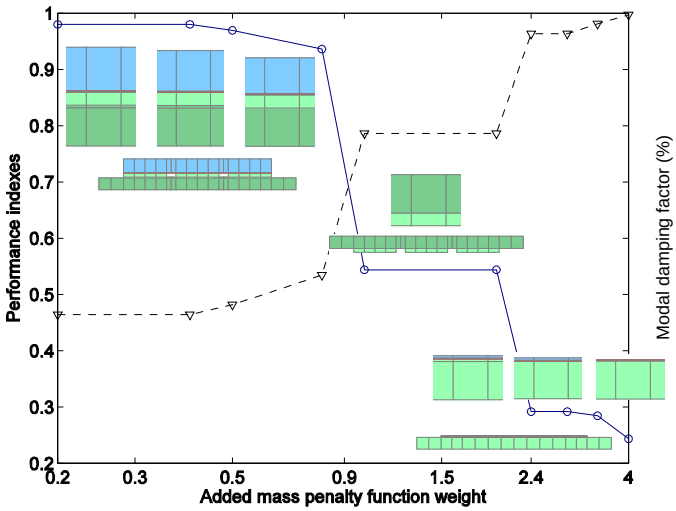

Figure 11 – Variation of damping performance index J_d (solid) and added mass penalty function J_m (dashed) for selected values of β.

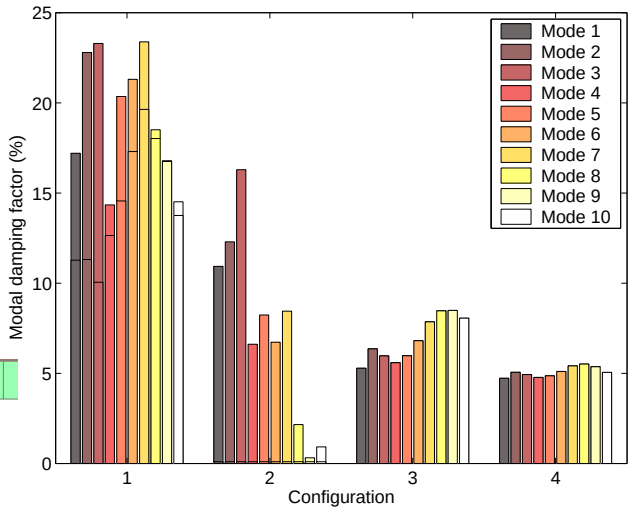

Figure 12 – Active, passive and hybrid damping for the first ten bending modes obtained with selected configurations.

The frequency and time responses of the treated beams are now compared to that of the base beam in Figures 13 and 14. In particular, from Figure 13, it can be noticed that all treatments are capable of greatly reducing the resonance amplitudes, except for the last three modes of the beam with the purely active damping treatment. The impulsive time response, shown in Figure 14, confirms that the response is well damped for all treatments when compared to the base beam. Indeed, the settling time of the base beam (2.5 seconds) is considerably reduced to 0.070, 0.045, 0.040 and 0.015 seconds by the active, free layer, constrained layer and active-passive damping treatments, respectively.

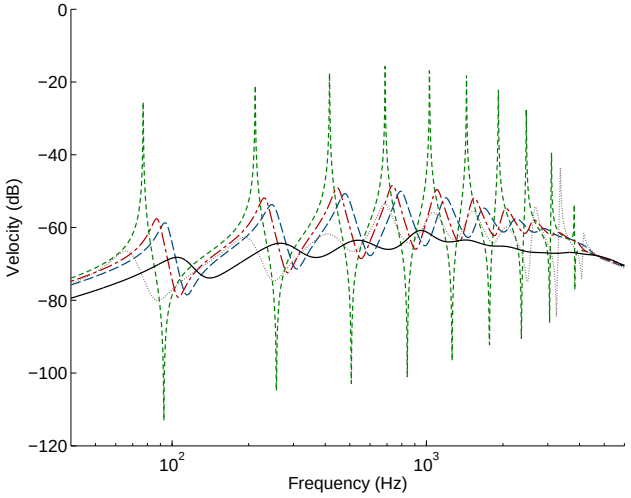

Figure 13 – Frequency response function for five selected configurations. - - -: base beam, – . –: passive free, – –: passive constrained, ···: active, ——: hybrid.

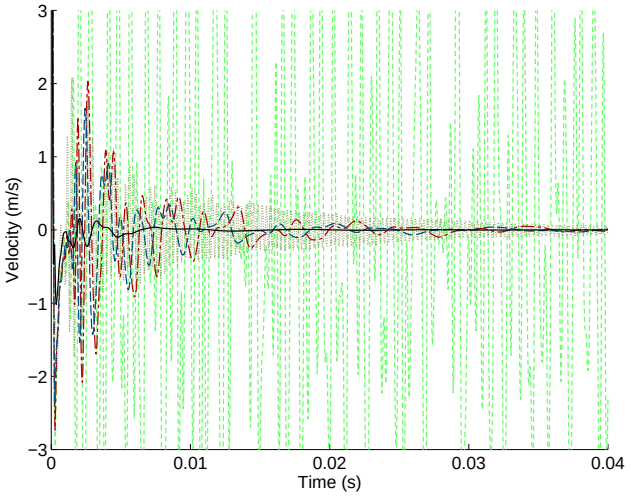

Figure 14 – Impulse response function for five selected configurations. - - -: base beam, – . –: passive free, – –: passive constrained, ···: active, ——: hybrid.

CONCLUDING REMARKS

This work has presented a methodology for the multiobjective geometric and topological optimization of hybrid active-passive damping treatments, composed by a passive viscoelastic layer sandwiched between a constraining and a spacer (or

stand-off) layer and an active layer of piezoelectric actuators. The optimization was performed using genetic algorithms operators together with an objective function that combines an average damping factor with the relative mass increase, weighted by an adjustable factor. The passive damping layer thickness and the relative position of the piezoelectric actuators were considered as design variables. Results have shown that a considerable improvement of damping performance is achievable with a controlled increase in the mass of the structure. In light of these results, future works are being directed to the experimental validation of selected active-passive configurations and their application to more complex structures.

ACKNOWLEDGMENTS

This research was supported by the State of São Paulo Research Foundation (FAPESP), through research grant 04/10255-7, which is gratefully acknowledged.

REFERENCES

Azvine, B., Tomlinson, G.R. and Wynne, R., 1995, "Use of active constrained-layer damping for controlling resonant vibration," Smart Materials and Structures, 4(1):1–6.

Baz, A. and Ro, J., 1994, "Concept and performance of active constrained layer damping treatments," Sound and Vibration Magazine, pp.18–21.

Begg, D.W. and Liu, X., 2000, "On simultaneous optimization of smart structures - part II: algorithms and example," Computer Methods in Applied Mechanics and Engineering, 184(1):25–37.

Goldberg, D., 1989, "Genetic algorithms in search, optimization, and machine learning," Addison-Wesley Pub. Co.

Houck, C.R., Joines, J. and Kay, M., 1995, "A genetic algorithm for function optimization: A matlab implementation", Technical Report NCSU-IE-TR-95-09, North Carolina State University, Raleigh, NC.

Huang, S.C., Inman, D.J. and Austin, E.M., 1996, "Some design considerations for active and passive constrained layer damping treatments," Smart Materials and Structures, 5(3):301–313.

Lam, M.J., Inman, D.J. and Saunders, W.R., 1998, "Variations of hybrid damping," In L.P. Davis (ed.), Smart Structures & Materials 1998: Passive Damping and Isolation, Vol.3327, pp.32–43, Bellingham (USA), SPIE.

Lesieutre, G.A. and Bianchini, E., 1995, "Time domain modeling of linear viscoelasticity using anelastic displacement fields," Journal of Vibration and Acoustics, 117(4):424–430.

Sadri, A.M., Wright, J.R. and Wynne, R.J., 1999, "Modelling and optimal placement of piezoelectric actuators in isotropic plates using genetic algorithms," Smart Materials and Structures, 8(4):490–498.

Steffen Jr., V., Rade, D.A. and Inman, D.J., 2000, "Using passive techniques for vibration damping in mechanical systems," Journal of the Brazilian Society of Mechanical Sciences, 22(3):411–421.

Trindade, M.A., 2006, "Reduced-order finite element models of viscoelastically damped beams through internal variables projection," Journal of Vibration and Acoustics, 128(4):501–508.

Trindade, M.A. and Benjeddou, A., 2002, "Hybrid active-passive damping treatments using viscoelastic and piezoelectric materials: review and assessment," Journal of Vibration and Control, 8(6):699–746.

Trindade, M.A., Benjeddou, A. and Ohayon, R., 2001, "Finite element modeling of hybrid active-passive vibration damping of multilayer piezoelectric sandwich beams – part 1: Formulation," International Journal for Numerical Methods in Engineering, 51(7):835–854.

Trindade, M.A., Benjeddou, A. and Ohayon, R., 2001, "Piezoelectric active vibration control of sandwich damped beams," Journal of Sound and Vibration, 246(4):653–677.

RESPONSIBILITY NOTICE